J. Fluid Mech. (2006), *vol.* 560, *pp.* 103–122. © 2006 Cambridge University Press
doi:10.1017/S0022112006000590 Printed in the United Kingdom

On imploding cylindrical and spherical shock waves in a perfect gas

By N. F. PONCHAUT, H. G. HORNUNG, D. I. PULLIN AND C. A. MOUTON

California Institute of Technology, Pasadena CA 91125, USA

(Received 4 July 2005 and in revised form 6 January 2006)

The problem of a cylindrically or spherically imploding and reflecting shock wave in a flow initially at rest is studied without the use of the strong-shock approximation. Dimensional arguments are first used to show that this flow admits a general solution where an infinitesimally weak shock from infinity strengthens as it converges towards the origin. For a perfect-gas equation of state, this solution depends only on the dimensionality of the flow and on the ratio of specific heats. The Guderley power-law result can then be interpreted as the leading-order, strong-shock approximation, valid near the origin at the implosion centre. We improve the Guderley solution by adding two further terms in the series expansion solution for both the incoming and the reflected shock waves. A series expansion, valid where the shock is still weak and very far from the origin, is also constructed. With an appropriate change of variables and using the exact shock-jump conditions, a numerical, characteristics-based solution is obtained describing the general shock motion from almost infinity to very close to the reflection point. Comparisons are made between the series expansions, the characteristics solution, and the results obtained using an Euler solver. These show that the addition of two terms to the Guderley solution significantly extends the range of validity of the strong-shock series expansion.

1. Introduction

The problem of an imploding shock wave is interesting from a fundamental gasdynamical point of view, and has important applications ranging from detonation and fusion initiation to the destruction of kidney stones. Guderley first investigated the problem by considering a cylindrical or spherical shock wave, initially at a very large radius, propagating inward through a perfect gas at rest and then reflecting from the axis or centre, see Guderley (1942).

Guderley considered only the case where the shock is already so intense that the strong form of the shock jump relations apply. For this case, he found a similarity solution, in which the shock radius is given by the time relative to the time at which it reaches the centre raised to some power smaller than unity, so that the shock strength becomes infinite at the centre. The value of this power is the same for the incoming and reflected shock waves. Since Guderley's work, this value has been recalculated with greater accuracy by several researchers. Hafner (1988) derived the equations in Lagrangian coordinates and used power series to solve these. By doing so, he was able to find the exponent value with a very high number of significant digits.

The problem was also studied by Chester (1954), Chisnell (1955), and Whitham (1958) with approximate methods, specifically geometrical shock dynamics. In their solutions, the exponent in the expression for the Mach number as a function of

https://doi.org/10.1017/S0022112006000590 Published online by Cambridge University Press

shock radius for the spherical case is exactly twice that for the cylindrical case. This approximate result differs from the exact solution by less than one percent. The geometrical shock dynamics method is both simple and intuitive while providing fairly accurate results.

More recently, Chisnell (1998) described the imploding shock problem analytically, along with the flow generated behind it, by making a few analytical assumptions. The exponent values that he found, using approximate equations, are fairly close to their exact values, which indicates that his descriptions are valid. Chisnell also investigated the converging shock behaviour when the specific heat ratio, γ, tends to 1 or to infinity. Finally, Lee (1967) used a quasi-similar approximation and was able to find the approximate flow behaviour even for finite Mach numbers. His solution agrees very well with the exact similarity solution.

Guderley suggested that the power-law solution should be extended as a power series. This would then permit relaxation of the strong-shock assumption, allowing solutions for an increased range of acceptable Mach numbers, valid farther from the point of reflection.

The aim of the present work is to identify a generalized imploding-shock problem using the full Rankine–Hugoniot shock-jump relations, and to obtain a power series solution both for the converging and reflected shocks in which the Guderley solution is the first term in the inner, strong-shock expansion. Such a solution would apply in and near the strong-shock limit. Also, we seek a series solution for the outer flow described by an initially infinitesimally weak shock at infinite radius as it propagates inward. Furthermore, we also aim to compute the full flow field for the generalized imploding shock using the method of characteristics. Finally, we want to compare the results with numerical simulations.

In the following sections we first carefully define the generalized imploding–reflecting shock flow. The problem will then be posed, dimensional analysis will be used to guide the solution strategy, and finally, the general equations will be given (§ 2). Then the Guderley solution will be interpreted and two additional terms will be added. A series expansion will also be formed for a very weak shock located very far from the reflection point (§ 3). An algorithm based on the method of characteristics, and designed to find the complete imploding shock solution from infinity to the origin, will be described (§ 4). Finally, some comparisons between expansions, characteristic solutions, and results from an Euler solver will be presented (§ 5). Note that the series expansion calculations involve very lengthy expressions. For this reason, only the method to solve the problem, and not the expressions themselves will be presented in this article. Further details are provided in Ponchaut (2005).

2. Problem definition

2.1. *General notation*

Consider the one-dimensional problem of a shock propagating, from infinity, through a stationary inviscid perfect gas, and reflecting at the origin. This shock can have either cylindrical ($\nu = 2$) or spherical symmetry ($\nu = 3$). The problem, as defined by Guderley (1942), has no characteristic length; the shock comes from infinity and reflects back to infinity. For the purposes of this paper, real gas effects and shock instabilities are not considered.

The independent variables in this problem are the radius, r, and the time, t. The shock position is given by $R_s(t)$ and its velocity is $U_s(t)$. The origin of the independent

https://doi.org/10.1017/S0022112006000590 Published online by Cambridge University Press

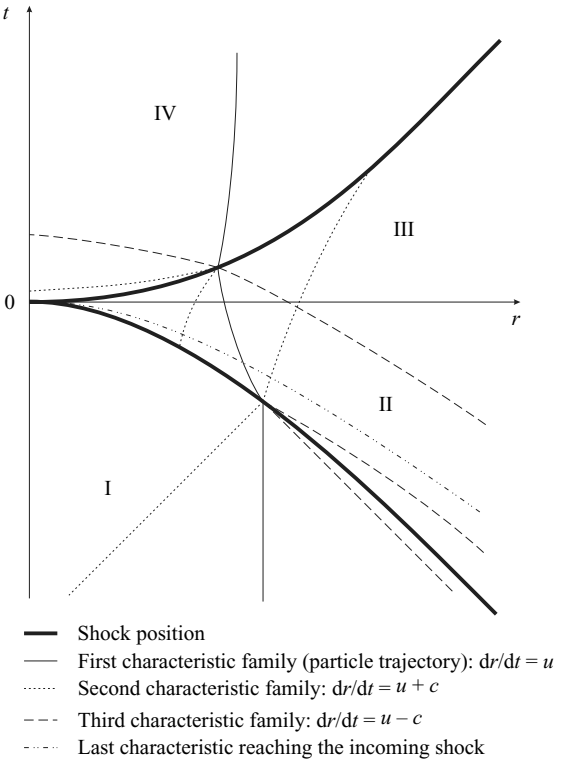


FIGURE 1. Sketch of the r–t diagram of the problem. The shock position is represented by the thick curves. The three different characteristic families are also shown. u and c are the local velocity and speed of sound of the flow, respectively.

variables is such that the shock reflects at $r = 0$ when $t = 0$, i.e.

$$R_s(0) = 0. \tag{2.1}$$

In this configuration, the incoming part of the shock is characterized by $t < 0$ and the reflected part, by $t > 0$. The medium is a perfect gas with a ratio of specific heats γ, and the flow upstream of the incoming shock is at rest with pressure P_I and density ρ_I. Note that the notation in this work, which is suitable for the series analysis, is slightly different from that chosen by Guderley.

The entire problem can be divided into four separate regions in the (r, t)-plane. Region I is the undisturbed flow ($t < 0$ and $r < R_s(t)$). In this region, the density and the pressure are constant and the flow is at rest. Region II corresponds to the flow behind the incoming shock ($t < 0$ and $r > R_s(t)$). Region III corresponds to the flow upstream of the reflected shock ($t > 0$ and $r > R_s(t)$). And, finally, region IV corresponds to the flow downstream of the reflected shock ($t > 0$ and $r < R_s(t)$). In the current notation, f_I refers to the value of f in region I, f_{II} to the value of f in region II, etc.

Figure 1 shows these four regions, as well as representative shapes of the different families of characteristics. First, a particle trajectory is shown as the thin solid curves. In region I, the flow is at rest and therefore the particle trajectories are just lines of constant r. After the incoming shock, the gas flows towards the centre but slows down in time due to the accumulation of mass. After the reflected shock, the flow is

https://doi.org/10.1017/S0022112006000590 Published online by Cambridge University Press

directed away from the centre and slows down to eventually come to rest when the pressure becomes constant in the whole domain. The second family of characteristics is defined by $\mathrm{d}r/\mathrm{d}t = u + c$ and is represented by dotted curves. In region I, these are straight lines representing waves moving at the speed of sound. After the incoming shock, they are deflected toward the centre and they stop at the shock. In fact, the second family of characteristics in region IV represents waves that travel faster than the shock and stop when they reach it. Finally, the third family of characteristics is defined by $\mathrm{d}r/\mathrm{d}t = u - c$ and is represented by dashed curves. In region I, these characteristics are also straight lines that describe waves moving at the speed of sound. They stop at the incoming shock since, in region II, they travel faster than the shock. The third family of characteristics in region II or III reaching the reflected shock are just deflected by the reflected shock. Note that the particular characteristic that reaches the shock at $t = 0$ is of special importance since it is the boundary of the domain that influences the incoming shock. This characteristic leads to singularities in the equations as explained in later sections.

Region I is already known and regions II, III and IV satisfy the Euler equations. Shock jump conditions must be satisfied along the boundaries between regions I and II and between regions III and IV. The variables must be continuous between regions II and III and finally, from physical arguments, the flow must have no velocity at the origin. It is important to note that the shock Mach number tends to infinity at the origin in the incoming case, but is finite in the reflected case. The reason for this is that, although the shock velocity is infinite at the origin, the speed of sound at the origin, in region III, is infinite as well.

2.2. *Dimensional analysis*

According to Buckingham's pi theorem, since we have seven variables, we can form four independent non-dimensional numbers. We will take these four non-dimensional parameters to be

$$\nu,\ \gamma,\ \theta = \frac{c_\mathrm{I} t}{R_\mathrm{s}},\ \eta = \frac{R_\mathrm{s}}{r},$$

where c_I is the speed of sound in the undisturbed region ($c_\mathrm{I} = \sqrt{\gamma P_\mathrm{I}/\rho_\mathrm{I}}$). These four non-dimensional variables are sufficient to describe the complete solution to the problem. This means that in (θ, η) coordinates, there exists a universal solution for a given γ and a given ν. The density, pressure, and velocity can be expressed as

$$\rho = \rho_\mathrm{I}\overline{\rho}(\nu, \gamma, \theta, \eta), \tag{2.2}$$

$$P = P_\mathrm{I}\overline{P}(\nu, \gamma, \theta, \eta), \tag{2.3}$$

$$u = c_\mathrm{I}\overline{u}(\nu, \gamma, \theta, \eta). \tag{2.4}$$

The shock motion can also be investigated by considering the velocity of the shock, $U_\mathrm{s} = \mathrm{d}R_\mathrm{s}/\mathrm{d}t$. Since the shock is located at $\eta = 1$, we have

$$U_\mathrm{s} = c_\mathrm{I} K^{(-1)}(\nu, \gamma, \theta), \tag{2.5}$$

where $K^{(-1)}$ is the inverse function of K with respect to $U_\mathrm{s}/c_\mathrm{I}$. K is an unknown function defined as

$$\theta = K\left(\nu, \gamma, \frac{U_\mathrm{s}}{c_\mathrm{I}}\right). \tag{2.6}$$

https://doi.org/10.1017/S0022112006000590 Published online by Cambridge University Press

This equation is useful since it is valid for all shock motions, regardless of the particular scaling of the problem. However, it is not convenient when direct predictions of the shock position are desired. In fact, (2.6) involves three variables (t, $R_s(t)$ and $U_s(t)$), and is a nonlinear differential equation for $R_s(t)$. This can be seen if we write (2.6) as

$$\frac{c_I t}{R_s(t)} = K\left(\nu, \gamma, \frac{1}{c_I}\frac{\mathrm{d}R_s(t)}{\mathrm{d}t}\right). \tag{2.7}$$

To find more suitable equations, we can drop one of the variables (t or U_s) and define a characteristic time, τ, such that $c_I\tau$ is the radius at which the incoming shock has a Mach number of 2 (arbitrary choice). In this case, we can show that we get the following expressions:

$$\frac{R_s}{c_I\tau} = F\left(\nu, \gamma, \frac{U_s}{c_I}\right), \tag{2.8}$$

$$\frac{R_s}{c_I\tau} = G\left(\nu, \gamma, \frac{t}{\tau}\right), \tag{2.9}$$

where

$$F(\nu, \gamma, -2) = 1, \tag{2.10}$$

$$G(\nu, \gamma, 0) = 0. \tag{2.11}$$

The series expansions will be written in the same form as (2.9). The functions F, G and K will be used to make comparisons between the solutions from the series expansions, the method of characteristics and Euler computations (§ 5.3).

3. Series expansion solutions

To obtain a simple solution, it is useful to find the limiting behaviours of the shock in the form of a series. Guderley obtained the first term of the expansion series solution close to the origin, for $r \ll c_I\tau$ (or equivalently, for $M_s \gg 1$). In the next subsections, we will first transform the equations to make them more suitable for solving the series expansion problems (§ 3.1). Guderley's solution will then be examined (§ 3.2) and extended with two additional terms (§ 3.3). Finally, series expansions will also be formed for the weak shock case, i.e. for $r \gg c_I\tau$, or for $M_s - 1 \ll 1$ (§ 3.4). These can be very useful as starting conditions when using a numerical method to find the solution in the entire domain.

3.1. *Initial change of variables*

Looking at figure 1, we see that the four regions have complicated shapes that are not known *a priori*. It is much easier to transform these regions into ones with fixed shapes to find out exactly where the shock jump conditions have to be applied. This can be done by making the change of variables

$$(t,\ r) \rightarrow (\eta,\ r),$$

where

$$\eta = \frac{R_s(t)}{r}. \tag{3.1}$$

The shock jump conditions now occur at $\eta = 1$ and under this change of variables, figure 1 is transformed into figure 2.

https://doi.org/10.1017/S0022112006000590 Published online by Cambridge University Press

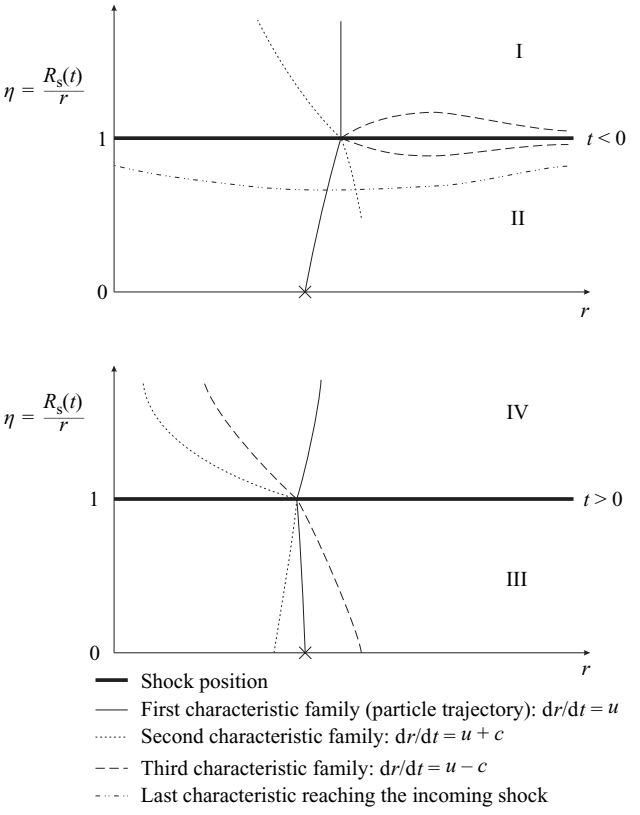


FIGURE 2. Sketch of the η–r diagram for the problem. The shock position is represented by the thick lines. The three different kinds of characteristics are shown as well. The crosses correspond to the same point in the (r, t) domain. Note the shape of the last characteristic reaching the incoming shock: in the η–r diagram, this particular characteristic reaches $r = 0$ at a finite $\eta < 1$. As will be shown in the next sections, the flow close to the origin is self-similar and the trajectory of this characteristic corresponds to a constant η that is different from unity. This particular characteristic leads to a singularity in the domain.

3.2. *Guderley's solution*

Guderley's work focused on the region close to $r = 0$ ($r \ll c_I \tau$). There, it can be assumed that between regions I and II, the strong-shock jump conditions are valid. Note that this assumption cannot be made for the reflected shock between III and IV. Although the reflected shock velocity tends to infinity when r tends to 0, its Mach number is finite since the speed of sound tends to infinity as well. Furthermore, Guderley hypothesized that under the strong-shock assumption, the shock position can be written as proportional to time raised to the power $n^{\pm}$. Using the notation introduced in (2.9), this means that

$$R_s(t) = c_I \tau \beta^{\pm} \left(\frac{|t|}{\tau} \right)^{n^{\pm}}, \tag{3.2}$$

where the superscript $\pm$ refers to a constant that has different values in the incoming and in the reflected cases, with $-$ and $+$ denoting the value in the incoming and in the reflected cases, respectively. To simplify the expressions in later sections, it is more

https://doi.org/10.1017/S0022112006000590 Published online by Cambridge University Press

convenient to write (3.2) as

$$R_s(t) = c_I \overline{\tau}_s \left(\frac{t}{\alpha^{\pm} \overline{\tau}_s} \right)^{n^{\pm}}, \tag{3.3}$$

where $\alpha^{\pm}$ is a constant that is chosen to be -1 for the incoming shock, and that has an unknown constant positive value α^{+} for the reflected shock, and where

$$\overline{\tau}_s = (\beta^{-})^{\frac{1}{1-n^{-}}} \tau. \tag{3.4}$$

The exponent $n^{\pm}$ is an unknown constant and, based on the work so far, its value is not necessarily the same in the incoming and in the reflected cases. Its value lies between 0 and 1 since $R_s(0) = 0$ and the speed of the shock tends to infinity as t tends to 0. From (3.3), we can find the shock velocity, which is given by

$$U_s(R_s) = c_I \frac{n^{\pm}}{\alpha^{\pm}} \left(\frac{t(R_s)}{\alpha^{\pm} \overline{\tau}_s} \right)^{n^{\pm}-1} = c_I \frac{n^{\pm}}{\alpha^{\pm}} \left(\frac{R_s}{c_I \overline{\tau}_s} \right)^{\frac{n^{\pm}-1}{n^{\pm}}}. \tag{3.5}$$

Since the shock position will only be accurate for $R_s \ll c_I \overline{\tau}_s$, the solution that we obtain will only be valid for small r. In addition, since the characteristics coming from the shock are only correct for small t (or small R_s), the solution is also only correct for $t \ll \overline{\tau}_s$.

The method to solve this simplified problem will be discussed in the following subsections. New shock jump conditions will first be written and new variables will be introduced (§ 3.2.1). From the resulting equations, the problem will be solved for $n^{\pm}$ and then for $\alpha^{\pm}$ (§ 3.2.2).

3.2.1. *Self-similar problem*

We first write the strong-shock jump conditions for the incoming case, which are

$$\rho_{II}(1, r) = \rho_I \frac{\gamma + 1}{\gamma - 1}, \tag{3.6}$$

$$P_{II}(1, r) = P_I \frac{2\gamma}{\gamma + 1} \left(\frac{U_s(R_s)_{\eta=1}}{c_I} \right)^2 = P_I \frac{2\gamma \left(n^{\pm}\right)^2}{\gamma + 1} \left(\frac{r}{c_I \overline{\tau}_s} \right)^{\frac{2(n^{\pm}-1)}{n^{\pm}}}, \tag{3.7}$$

$$u_{II}(1, r) = \frac{2}{\gamma + 1} U_s(R_s)_{\eta=1} = -c_I \frac{2n^{\pm}}{\gamma + 1} \left(\frac{r}{c_I \overline{\tau}_s} \right)^{\frac{n^{\pm}-1}{n^{\pm}}}, \tag{3.8}$$

where we used the fact that $(R_s)_{\eta=1} = r$ and that for the incoming case $\alpha^{-} = -1$. These equations suggest that we try a solution of the form

$$\rho(\eta, r) = \rho_I \rho_1(\eta), \tag{3.9}$$

$$P(\eta, r) = P_I P_1(\eta) \left(\frac{n^{\pm}}{\alpha^{\pm}} \right)^2 \left(\frac{r}{c_I \overline{\tau}_s} \right)^{\frac{2(n^{\pm}-1)}{n^{\pm}}}, \tag{3.10}$$

$$u(\eta, r) = c_I u_1(\eta) \frac{n^{\pm}}{\alpha^{\pm}} \left(\frac{r}{c_I \overline{\tau}_s} \right)^{\frac{n^{\pm}-1}{n^{\pm}}}, \tag{3.11}$$

where $\rho_1(\eta)$, $P_1(\eta)$, and $u_1(\eta)$ are unknown functions of η only. The subscripts 1, 2, and 3 denote the first, second, and third terms in the series expansions. Since, when this solution form is substituted into the Euler equations, there is no longer a dependence on r, the assumed form of the variables is acceptable and the problem becomes self-similar.

https://doi.org/10.1017/S0022112006000590 Published online by Cambridge University Press

Once again, we have not made any assumptions about the value of the exponent $n^{\pm}$. Using the change of variables defined earlier, the continuity conditions between regions II and III can be written as

$$\rho_{1,\mathrm{III}}(0) = \rho_{1,\mathrm{II}}(0), \tag{3.12}$$

$$P_{1,\mathrm{III}}(0)\left(\frac{n^+}{\alpha^+}\right)^2\left(\frac{r}{c_{\mathrm{I}}\overline{\tau}_{\mathrm{s}}}\right)^{\frac{2(n^+-1)}{n^+}} = P_{1,\mathrm{II}}(0)\left(n^-\right)^2\left(\frac{r}{c_{\mathrm{I}}\overline{\tau}_{\mathrm{s}}}\right)^{\frac{2(n^--1)}{n^-}}, \tag{3.13}$$

$$u_{1,\mathrm{III}}(0)\frac{n^+}{\alpha^+}\left(\frac{r}{c_{\mathrm{I}}\overline{\tau}_{\mathrm{s}}}\right)^{\frac{n^+-1}{n^+}} = -u_{1,\mathrm{II}}(0)\,n^-\left(\frac{r}{c_{\mathrm{I}}\overline{\tau}_{\mathrm{s}}}\right)^{\frac{n^--1}{n^-}}. \tag{3.14}$$

These conditions must be satisfied for all r. This is only possible if we impose the condition that $n^{\pm} = n^+ = n^- = n$. Finally, as noted before, the full Rankine–Hugoniot shock jump conditions are used between regions III and IV since the reflected shock Mach number is finite.

Using the definitions introduced in this subsection, the resulting equations form a non-linear system of differential equations that can be further simplified by applying a final change of variables:

$$\phi_1(\eta) = \eta^{1/n}u_1(\eta), \tag{3.15}$$

$$\pi_1(\eta) = \frac{\eta^{2/n}P_1(\eta)}{\gamma\rho_1(\eta)\left[1-\phi_1(\eta)\right]}, \tag{3.16}$$

which leads to a system of differential equations of the form

$$\frac{\mathrm{d}\phi_1(\eta)}{\mathrm{d}\log\eta} = f_1(\phi_1(\eta), \pi_1(\eta)), \tag{3.17}$$

$$\frac{\mathrm{d}\pi_1(\eta)}{\mathrm{d}\log\eta} = g_1(\phi_1(\eta), \pi_1(\eta)), \tag{3.18}$$

$$\frac{\mathrm{d}\rho_1(\eta)}{\mathrm{d}\log\eta} = h_1(\phi_1(\eta), \pi_1(\eta)). \tag{3.19}$$

It is easier to treat ϕ_1 as the independent variable rather than η. We then obtain the following two differential equations:

$$\frac{\mathrm{d}\pi_1(\phi_1)}{\mathrm{d}\phi_1} = \frac{g_1(\phi_1, \pi_1(\phi_1))}{f_1(\phi_1, \pi_1(\phi_1))}, \tag{3.20}$$

$$\frac{\mathrm{d}\log\eta(\phi_1)}{\mathrm{d}\phi_1} = \frac{1}{f_1(\phi_1, \pi_1(\phi_1))}. \tag{3.21}$$

Along with these equations, a first integral can be found:

$$\rho_1(\phi_1) = C\left[\frac{\pi_1(\phi_1)^n}{\eta(\phi_1)^2}\left(1-\phi_1\right)^{\frac{2(1-n)+n\nu}{\nu}}\right]^{\frac{\nu}{n\nu(\gamma-1)-2(1-n)}}, \tag{3.22}$$

where C is a constant that takes a different value in each region. The problem is now relatively easy to solve since (3.20) can first be considered alone to solve for $\pi_1(\phi_1)$. Then, (3.21) can be integrated to find $\eta(\phi_1)$. $\rho_1(\phi_1)$ is obtained using the first integral (3.22).

3.2.2. *Discussion and solution*

First, consider the limiting values of the problem. In region II, just downstream of the shock, $\phi_{1,\mathrm{II}}$ and $\pi_{1,\mathrm{II}}$ are given exactly by the shock jump conditions. At the

https://doi.org/10.1017/S0022112006000590 Published online by Cambridge University Press

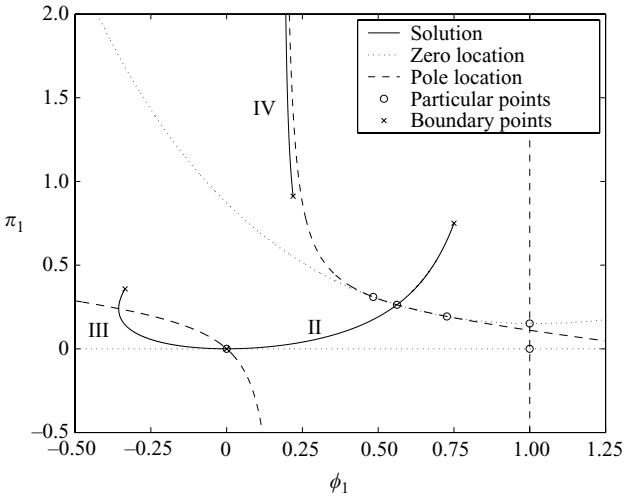


FIGURE 3. Zero and pole locations of the right-hand side of the $\pi_1'(\phi_1)$ equation (3.20), for $\nu = 3$, $\gamma = 5/3$, and $n = 0.68838$. The circles are the particular points that are intersections of the zero and the pole curves. The solution is represented by the solid curve and the crosses show the boundaries of the regions.

junction between II and III, ρ_1, P_1, and u_1 are continuous and finite, meaning that, since η tends to 0, ϕ_1 and π_1 also tend to 0 at the junction (see (3.15) and (3.16)). Finally in region IV, when η tends to infinity, $P_{1,\mathrm{IV}}$ must be finite, meaning that $\pi_{1,\mathrm{IV}}(1-\phi_{1,\mathrm{IV}})$ must also tend to infinity. In addition, ϕ_1 cannot change sign within a region, and $\pi_1(1-\phi_1)$ must always remain positive. For any given case, ν and γ are fixed. For each value of n, we can plot, in the (ϕ_1, π_1)-plane, the zeros and poles of the right-hand side of (3.20) and (3.21). Figure 3 shows these for $\pi_1'(\phi_1)$ (3.20).

In region II, the solution trajectory in the (ϕ_1, π_1) domain must go from the initial point to (0, 0). Along this trajectory, the variables must be continuous. This is only possible if the trajectory crosses a pole while simultaneously crossing a zero and vice-versa. In fact, it can be shown that if this is not the case, the solution will not be smooth within the region. It is conceptually easy to find n since it corresponds to the value at which the trajectory crosses one of the circled points in figure 3. It is important to note that the singular point corresponds to a point on the limiting characteristic, which is the characteristic that reaches $r = 0$ at $t = 0$ and is represented in the characteristic sketches by a dash-dot-dot curve.

Consider now the trajectory in region IV. By examining (3.20), we see that the only way $\phi_{1,\mathrm{IV}}(\eta)/\eta^{1/n}$ can tend to infinity while keeping $\pi_{1,\mathrm{IV}}(\eta)[1-\phi_{1,\mathrm{IV}}(\eta)]/\eta^{2/n}$ finite, is for the trajectory to become tangent to the pole curve around its singularity. This condition leads to a specific value of α^+ (α^- being -1). As an example, figure 3 represents the solution trajectory for $\nu = 3$ and $\gamma = 5/3$, in the (ϕ_1, π_1)-plane, along with the corresponding pole and zero curves of the $\pi_1'(\phi_1)$, equation (3.20). Note that in this case, $\pi_1'(\phi_1)$ becomes infinite and changes sign within region III.

Finally, as discussed in § 2.2, τ is a characteristic time. The ratio $\overline{\tau}_s/\tau$ and the constant $\beta^{\pm}$, in (3.4), cannot be evaluated using this expansion series method. The entire problem has to be computed using a different method and the constants are determined so that the shock trajectory fits the expansion. This process will be explained in more detail in § 4.

https://doi.org/10.1017/S0022112006000590 Published online by Cambridge University Press

3.3. *Strong-shock series expansion*

Guderley's solution described in § 3.2 is only valid for very strong shocks ($M^2 \gg 1$ or $R_s \ll c_1\tau$). It is therefore useful to extend the solution in the form of a series expansion so that the approximate solution remains valid over a wider range of Mach numbers as was suggested by Guderley (1942). The way to do this is to extend (3.3) and to assume a shock position equation of the form

$$R_s(t) = c_1\overline{\tau}_s\left(\frac{t}{\alpha^{\pm}\overline{\tau}_s}\right)^n\left[1 + a_2^{\pm}\left(\frac{t}{\alpha^{\pm}\overline{\tau}_s}\right)^{i_2} + a_3^{\pm}\left(\frac{t}{\alpha^{\pm}\overline{\tau}_s}\right)^{i_3} + \mathrm{HOT}\right], \tag{3.23}$$

where $i_k < i_{k+1}$ and where HOT represents all the higher-order terms. Essentially, each additional term partially corrects for the fact that, for finite Mach numbers, the strong shock solution is not exact. Although it involves lengthy calculations, the method to find the values of i_k is straightforward. First, the shock location is expanded in terms of a power series in t. The shock jump conditions between regions I and II, and the variables ρ, P, and u are expanded in a series as well. A new system of differential equations is written for each term. These systems of equations are singular at exactly the same points as those found in the Guderley strong-shock solution. Each system must possess a coefficient $a_k^{\pm}$ with a value such that the singularity is avoided. If the exponents i_k are not correct, some systems of equations will not have a coefficient available to avoid infinite derivatives at the corresponding singular point. Performing all the calculations, it can be shown that $i_k = 2(k-1)(1-n)$.

Substituting the appropriate exponents into (3.23) produces a shock motion given by

$$R_s(t) = c_1\overline{\tau}_s\left(\frac{t}{\alpha^{\pm}\overline{\tau}_s}\right)^n\left[1 + a_2^{\pm}\left(\frac{t}{\alpha^{\pm}\overline{\tau}_s}\right)^{2(1-n)} + a_3^{\pm}\left(\frac{t}{\alpha^{\pm}\overline{\tau}_s}\right)^{4(1-n)} + \mathrm{HOT}\right]. \tag{3.24}$$

Using standard series inversion techniques, we obtain

$$t(R_s) = \alpha^{\pm}\overline{\tau}_s\left(\frac{R_s}{c_1\overline{\tau}_s}\right)^{1/n}\left[1 - \frac{a_2^{\pm}}{n}\left(\frac{R_s}{c_1\overline{\tau}_s}\right)^{\frac{2(1-n)}{n}} + \frac{(a_2^{\pm})^2(5-3n) - 2na_3^{\pm}}{2n^2}\left(\frac{R_s}{c_1\overline{\tau}_s}\right)^{\frac{4(1-n)}{n}} + \mathrm{HOT}\right]. \tag{3.25}$$

Using the same technique as used by Guderley, a series expansion can be written for the full Rankine–Hugoniot shock jump conditions between regions I and II and between regions III and IV, as well as for the continuity conditions between regions II and III. These series are in terms of $r/(c_1\overline{\tau}_s)$ and lead us to try series solutions of the form

$$\rho(\eta, r) = \rho_1\rho_1(\eta)\left[1 + \rho_2(\eta)\left(\frac{r}{c_1\overline{\tau}_s}\right)^{\frac{2(1-n)}{n}} + \rho_3(\eta)\left(\frac{r}{c_1\overline{\tau}_s}\right)^{\frac{4(1-n)}{n}} + \mathrm{HOT}\right], \tag{3.26}$$

$$P(\eta, r) = P_1P_1(\eta)\left(\frac{n}{\alpha^{\pm}}\right)^2\left(\frac{r}{c_1\overline{\tau}_s}\right)^{\frac{2(n-1)}{n}} \times\left[1 + P_2(\eta)\left(\frac{r}{c_1\overline{\tau}_s}\right)^{\frac{2(1-n)}{n}} + P_3(\eta)\left(\frac{r}{c_1\overline{\tau}_s}\right)^{\frac{4(1-n)}{n}} + \mathrm{HOT}\right], \tag{3.27}$$

https://doi.org/10.1017/S0022112006000590 Published online by Cambridge University Press

$$u(\eta, r) = c_{\mathrm{I}} u_1(\eta) \frac{n}{\alpha^{\pm}} \left(\frac{r}{c_{\mathrm{I}} \overline{\tau}_{\mathrm{s}}} \right)^{\frac{n-1}{n}} \times \left[1 + u_2(\eta) \left(\frac{r}{c_{\mathrm{I}} \overline{\tau}_{\mathrm{s}}} \right)^{\frac{2(1-n)}{n}} + u_3(\eta) \left(\frac{r}{c_{\mathrm{I}} \overline{\tau}_{\mathrm{s}}} \right)^{\frac{4(1-n)}{n}} + \mathrm{HOT} \right]. \tag{3.28}$$

When these series are introduced into the Euler equations, the new expressions lead to a new series of equations. The way to solve this new problem is to add one term at a time into the series. Assuming that the first $(k-1)$ terms are solved, an additional term can be added to all the series (introducing a new coefficient $a_k^{\pm}$ in the process). This leads to a series of systems of Euler equations. Given that the first $(k-1)$ systems in the series have already been solved, only the kth system needs to be considered. Performing appropriate changes of variables, the following system can be written:

$$\frac{\mathrm{d}}{\mathrm{d}\phi_1} \begin{pmatrix} \phi_k(\phi_1) \\ \pi_k(\phi_1) \\ \psi_k(\phi_1) \end{pmatrix} = \boldsymbol{M}_k \begin{pmatrix} \phi_k(\phi_1) \\ \pi_k(\phi_1) \\ \psi_k(\phi_1) \end{pmatrix} + a_k^{\pm} \boldsymbol{b}_k + \boldsymbol{c}_k, \tag{3.29}$$

where $\boldsymbol{M}_k$ is a matrix, and where $\boldsymbol{b}_k$ and $\boldsymbol{c}_k$ are vectors. These are singular at the limiting characteristic in region II and at $r = 0$ in region IV. To solve the system, a_k^- and a_k^+ are chosen to remove the singular behaviour in region II and in region IV, respectively.

Knowing the values of the coefficient $a_k^{\pm}$, the function G defined in § 2.2 can be obtained:

$$\frac{R_{\mathrm{s}}}{c_{\mathrm{I}} \tau} = G\left(\nu, \gamma, \frac{t}{\tau}\right) = \frac{\overline{\tau}_{\mathrm{s}}}{\tau} \left(\frac{1}{\alpha^{\pm}(\overline{\tau}_{\mathrm{s}}/\tau)} \frac{t}{\tau} \right)^n \left[1 + a_2^{\pm} \left(\frac{1}{\alpha^{\pm}(\overline{\tau}_{\mathrm{s}}/\tau)} \frac{t}{\tau} \right)^{2(1-n)} + a_3^{\pm} \left(\frac{1}{\alpha^{\pm}(\overline{\tau}_{\mathrm{s}}/\tau)} \frac{t}{\tau} \right)^{4(1-n)} + \mathrm{HOT} \right]. \tag{3.30}$$

The non-dimensional functions F and K can be written in a similar form. Note that in (3.30), the ratio $\overline{\tau}_{\mathrm{s}}/\tau$ is constant for a given symmetry and a given γ, and cannot be obtained using series expansions. This ratio can only be obtained by solving the full problem (see § 4).

Note that, based on the results obtained, the series presented in this section seem to be at least asymptotic. Their convergence was not studied however. More details about the equations involved in the calculations can be found in Ponchaut (2005).

3.4. *Weak-shock series expansion*

In Guderley's problem, the shock is supposed to come from infinity, to travel up to $r = 0$, and then to bounce back to infinity. It is therefore also interesting to look for an expansion solution when the shock is still weak and far from the origin. This can only be done in the incoming shock case. In fact, in the reflected shock case, the full history of the flow is required and no analytic behaviour can easily be obtained. If we construct a series expansion similar to what was done in §§ 3.2 and 3.3, but expand the solution around (r, t) tending to $(\infty, -\infty)$ rather than $(0, 0)$, we get

$$\frac{R_{\mathrm{s}}}{c_{\mathrm{I}} \tau} = \frac{\overline{\tau}_{\mathrm{w}}}{\tau} \left[-\frac{\tau}{\overline{\tau}_{\mathrm{w}}} \frac{t}{\tau} + \sqrt{-\frac{\tau}{\overline{\tau}_{\mathrm{w}}} \frac{t}{\tau}} - \frac{19 + 3\gamma}{16(\gamma + 1)} \log\left(-\frac{\tau}{\overline{\tau}_{\mathrm{w}}} \frac{t}{\tau} \right) + \bar{t}_0 + \mathrm{HOT} \right], \tag{3.31}$$

https://doi.org/10.1017/S0022112006000590 Published online by Cambridge University Press

in the cylindrical case, and

$$\frac{R_s}{c_1\tau} = \frac{\overline{\tau}_w}{\tau}\left[-\frac{\tau}{\overline{\tau}_w}\frac{t}{\tau} + \log\left(-\frac{\tau}{\overline{\tau}_w}\frac{t}{\tau}\right) + \bar{t}_0 + \frac{\log\left(-\dfrac{\tau}{\overline{\tau}_w}\dfrac{t}{\tau}\right)}{-\dfrac{\tau}{\overline{\tau}_w}\dfrac{t}{\tau}} + \frac{\bar{t}_0 + \dfrac{\gamma+5}{\gamma+1}}{-\dfrac{\tau}{\overline{\tau}_w}\dfrac{t}{\tau}} + \mathrm{HOT}\right] \quad (3.32)$$

in the spherical case.

In the weak-shock expansion, both the ratio $\overline{\tau}_w/\tau$ and the constant $\bar{t}_0$ are unknown and cannot be found using series expansion. Note that $\bar{t}_0$ acts like a time shift that allows the shock to reach the origin at $t = 0$.

4. Incoming shock complete solution

In the previous section, we investigated the limiting behaviours of the problem and we obtained solutions that included unknown values. These particular values are $\overline{\tau}_s/\tau$ in the strong-shock expansion, $\overline{\tau}_w/\tau$ and $\bar{t}_0$ in the weak-shock expansion. These can only be determined with a complete calculation of the incoming shock problem. For that purpose, as well as to obtain the complete incoming shock solution, a first-order-accurate program based on the method of characteristics was written.

Since the program has to be able to compute the flow starting at $R_s \gg c_1\tau$ and ending at $R_s \ll c_1\tau$, computing the solution in real space (r, t) would be very inconvenient. To avoid that, the following change of variables is performed:

$$\theta = \frac{c_1 t}{R_s(t)}, \quad \eta = \frac{R_s(t)}{r}.$$

With this change of variables, the infinite domain becomes a square-bounded domain with θ ranging from -1 to 0 and η ranging from 0 to 1 (see figure 4). The reason for introducing θ follows logically from (2.6). In fact, in solving the problem, we will naturally find the unknown function $\theta = K(\nu, \gamma, U_s/c_1)$.

In § 3.2.1, we saw that close to the origin, the shock jump conditions give a finite density behind the shock, but the pressure, the velocity and the shock speed tend to infinity. For a shock very close to the origin, we have that

$$P_{II}(1, \theta) \propto R_s^{\frac{2(n-1)}{n}} \propto \frac{1}{\theta^2}, \quad (4.1)$$

$$u_{II}(1, \theta) \propto R_s^{\frac{n-1}{n}} \propto \frac{1}{\theta}, \quad (4.2)$$

$$U_s(\theta) \propto R_s^{\frac{n-1}{n}} \propto \frac{1}{\theta}. \quad (4.3)$$

To avoid any singular values in the computational domain, the following new variables are used:

$$\overline{P}(\eta, \theta) = \theta^2 \frac{P_{II}(\eta, \theta)}{P_I}, \qquad \overline{u}(\eta, \theta) = \theta \frac{u_{II}(\eta, \theta)}{c_I},$$

$$\overline{c}(\eta, \theta) = \frac{\theta}{c_I}\sqrt{\frac{\gamma P_{II}(\eta, \theta)}{\rho_{II}(\eta, \theta)}}, \qquad \overline{U}_s(\theta) = \theta \frac{U_s(\theta)}{c_I}.$$

Using this last change of variables, the characteristics equations can be written and the problem can be solved for $\overline{P}(\eta, \theta)$, $\overline{u}(\eta, \theta)$, $\overline{c}(\eta, \theta)$, and $\overline{U}_s(\theta)$.

https://doi.org/10.1017/S0022112006000590 Published online by Cambridge University Press

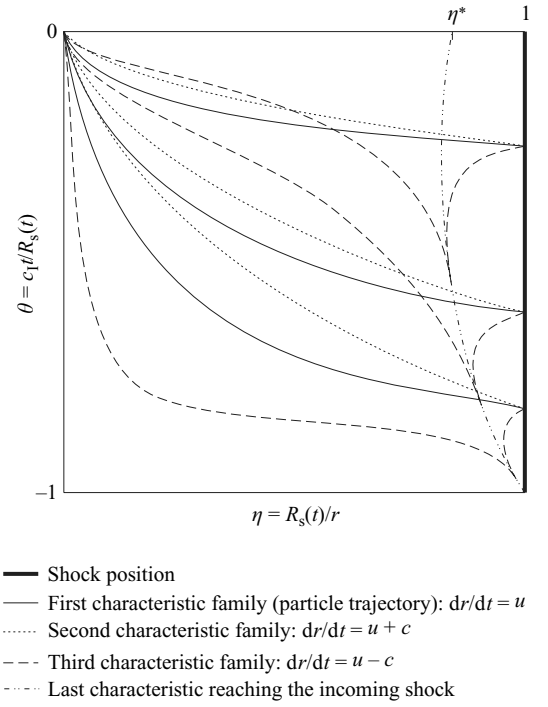


FIGURE 4. Sketch of the η–θ diagram for the problem in region II. The shock position is represented by the thick line. Its motion starts at $\theta = -1$ and ends at $\theta = 0$. The three different kinds of characteristics are also shown. η^* is the value of η at which there is a singularity in the strong-shock series expansion. Very close to the origin the flow is self-similar and the non-dimensional trajectory of the singular characteristic $\eta^* = R_s/r^*$ approaches a finite value that is different from unity, when $t \to 0$.

As seen in figure 4, all the third-family characteristics influencing the incoming shock start at $(\theta, \eta) = (-1, 1)$. This means that the whole problem is defined at that singular point. Since it is impossible to start there, the program needs to start at $\theta + 1 \ll 1$ and the weak-shock series expansion can be used as the starting flow. Note that at finite but small $\theta + 1$, the third-family characteristics that influence the shock do not merge to a point; they do however remain within a very narrow range of η. Since all the characteristics going to the shock start from this narrow range, we have to be able to add characteristics inside the domain. If, during the computation, the spacing of two successive characteristics of the same family becomes excessive, a new characteristic is initiated between them. This is done by creating a node that is interpolated along a characteristic of the other family. To maintain accuracy during this process, the interpolation has to be of an order that is at least as high as the order of the characteristic computations.

As previously mentioned, to start the computation, the weak-shock solution is used with a value of θ that is close to -1. In (η, θ) coordinates, $\bar{t}_0$ is the only unknown constant appearing in the starting conditions. If $\bar{t}_0$ had the correct value, the problem could theoretically be integrated up to the reflection point and θ would tend to 0 at the same time as c_I/U_s. If the guessed value of $\bar{t}_0$ is too low, the integration leads to a shock radius that tends to 0 before time reaches 0. This means that θ will tend to infinity. On the other hand, if the value of $\bar{t}_0$ is too high, the time tends to 0 before

https://doi.org/10.1017/S0022112006000590 Published online by Cambridge University Press

the shock radius and θ tends to 0 for a finite value of c_I/U_s. A bisection method is used to obtain the correct value of $\bar{t}_0$.

To find the ratios $\overline{\tau}_w/\tau$ and $\overline{\tau}_s/\tau$, the following equation is integrated starting at a Mach number close to 1:

$$\frac{1}{c_I}\frac{dR_s}{dt} = \frac{U_s(\theta)}{c_I} = \frac{\overline{U}_s(\theta)}{\theta} = \frac{\overline{U}_s(c_I t/R_s)}{c_I t/R_s}. \tag{4.4}$$

The initial conditions (R_s, t) can be random and the value of $\overline{\tau}_w$ is arbitrarily chosen, since the unknown ratios are independent of these values. Once integrated, (4.4) gives $R_s(t)/c_I$. From there, it is easy to find the functions F and G used in (2.8) and (2.9), respectively. Finally, τ can be obtained by using $\tau = R_s^\star/c_I$, where $R_s^\star$ is the radius at which the incoming shock has a Mach number of 2. Fitting the strong-shock expansion result with the integrated solution, we finally get $\overline{\tau}_s$. The ratios $\overline{\tau}_w/\tau$ and $\overline{\tau}_s/\tau$ can then be evaluated.

It is important to note that $\bar{t}_0$ and the two ratios were not found with a high degree of accuracy since the integration performed was only first order and that, for example, the constant in the initial conditions does not appear in any dominant terms. Even though the accuracy is not high, the bisection method has to find the appropriate $\bar{t}_0$ value with a high number of significant digits so that the characteristics can be computed up to a value of θ that is close to 0. In other words, we must find very accurately a value of $\bar{t}_0$ that is consistent with our integration scheme, even though the value of $\bar{t}_0$ itself was not very accurate.

5. Results

In this section, the series expansion calculations will be compared to the characteristics results. In addition, some comparisons will include computational fluid dynamic calculations of the Euler equations made in the AMRITA environment, see Quirk (1998).

The strong-shock series expansion coefficients were calculated using 2000 points in region II, 2000 points in region III, and 1000 points in region IV. We will compare some aspects of the results obtained by each method in the following sections. First, the characteristics will be shown in the (η, θ)-plane (§ 5.1). The density, the pressure, and the velocity distributions will be compared for Euler calculations and the series expansions (§ 5.2). Finally, the non-dimensional functions F, G, and K that were defined in § 2.2 will be compared between the methods (§ 5.3). In addition, some values of the constants in the expansion series are presented in table 1, along with an estimate of the number of significant digits.

5.1. *Characteristic results*

Figure 5 shows one set of the characteristic results and illustrates the basic shapes of the second and third characteristic family. This calculation has cylindrical symmetry and a specific heat ratio, γ, of 1.4. The calculations were started at $\theta = -0.995$ and were stopped at $\theta = -0.0338$, which corresponds to shock Mach numbers ranging from 1.00257 to 24.6 or to a shock radius ratio between the final and the initial points of about 2×10^{-12}. In the figure, characteristics of the second family are represented with dotted curves and characteristics of the third family are represented with dashed curves. The characteristic that separates the portion of the flow in region II that influences the shock from the rest of the region is clearly distinguishable. The limit of this particular characteristic for θ tending to 0 is given in the strong-shock expansion

https://doi.org/10.1017/S0022112006000590 Published online by Cambridge University Press

https://doi.org/10.1017/S0022112006000590 Published online by Cambridge University Press

γ	n	α^+	a_2^-	a_2^+	a_3^-	a_3^+	η^*	$\bar{t}_0$	$\frac{\overline{\tau}_s}{\tau}$	$\frac{\overline{\tau}_w}{\tau}$
				Cylindrical symmetry						
1.2	0.86116302390	6.099957294	−0.56495331	21.4953	5.5264	−106.97	0.8797191058	0.7212	195.6	30.66
1.4	0.835323191953	2.8156109349	0.2335140	8.92588	1.0608	−52.646	0.85129137696	0.6470	49.26	23.39
5/3	0.8156229691667	1.6947147269	0.5004547	4.391459	−0.1756	−22.670	0.830529251753	0.5678	26.34	17.87
				Spherical symmetry						
1.2	0.75714181478	6.431231558	−0.6267725	50.4650	9.13	−613.7	0.91041281789	−0.7612	20.93	3.119
1.4	0.717174501488	2.688492680	0.275784	16.614985	2.59	−200.2	0.88628918681	−0.7052	9.933	2.727
5/3	0.6883740859496	1.5478188813	0.621289	7.06248	4.774	−16.5	0.867641792579	−0.6426	7.042	2.387

TABLE 1. Values of the different constants. The numbers are displayed with an estimated number of significant digits. These estimates were obtained by computing each value with varying integration step sizes.

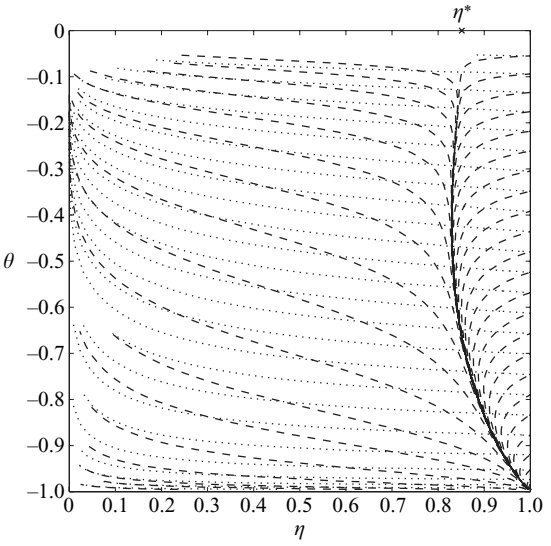


FIGURE 5. Second and third characteristic families in the cylindrical shock case for $\gamma = 1.4$. Dotted and dashed curves represent characteristics of the second and the third families, respectively. The cross represents the limit of the last characteristic reaching the incoming shock. This limit corresponds to the value of η at the singular point in region II in the strong-shock series expansion.

calculation since it corresponds to the value of η at the singularity (η^*). This limit is represented by a cross in the figure. Due to the singular behaviour of the characteristics close to $\eta = 0$ and to $\theta = 0$, the characteristics could not be computed in the entire domain and were therefore cropped.

5.2. *ρ, P, and u distribution*

Comparisons of the flow properties were made between the strong-shock series expansion and Euler calculations. The variables ρ, P, u, and t are normalized by ρ_I, $\rho_I|U_s(r)^-|^2$, $|U_s(r)^-|$, and $|t_s(r)^-|$, respectively. In these expressions, $U_s(r)^-$ is the speed of the incoming shock when it crosses the radius r, and $t_s(r)^-$ is the time at which that occurs.

Comparisons are made in the spherical case, for $\gamma = 1.4$. The shock was initiated with a Mach number of 5 and the variables were taken at a radius 10 times smaller than the initial radius where the Mach number was 12.4.

Figure 6 shows the variation over time of the normalized density, pressure and velocity. Guderley's solution is accurate for very high Mach numbers, but at the current Mach numbers, it shows some discrepancies with the Euler results. Most of these discrepancies appear in the density and the pressure distributions. The discrepancies are greatly reduced when two terms are added to the expansion. As explained previously, the shock series expansions are accurate for a low shock radius ($R_s \ll c_I\tau$). But this also means that the flow properties at a given small radius will only be valid for small times ($t \ll \tau$).

5.3. *The non-dimensional functions F, G, and K*

The functions F, G, and K were introduced in § 2.2. Given the symmetry of the problem, ν, and specific heat ratio, γ, these functions are fully defined. They are particularly useful since they describe all possible shock trajectories. The weak and

https://doi.org/10.1017/S0022112006000590 Published online by Cambridge University Press

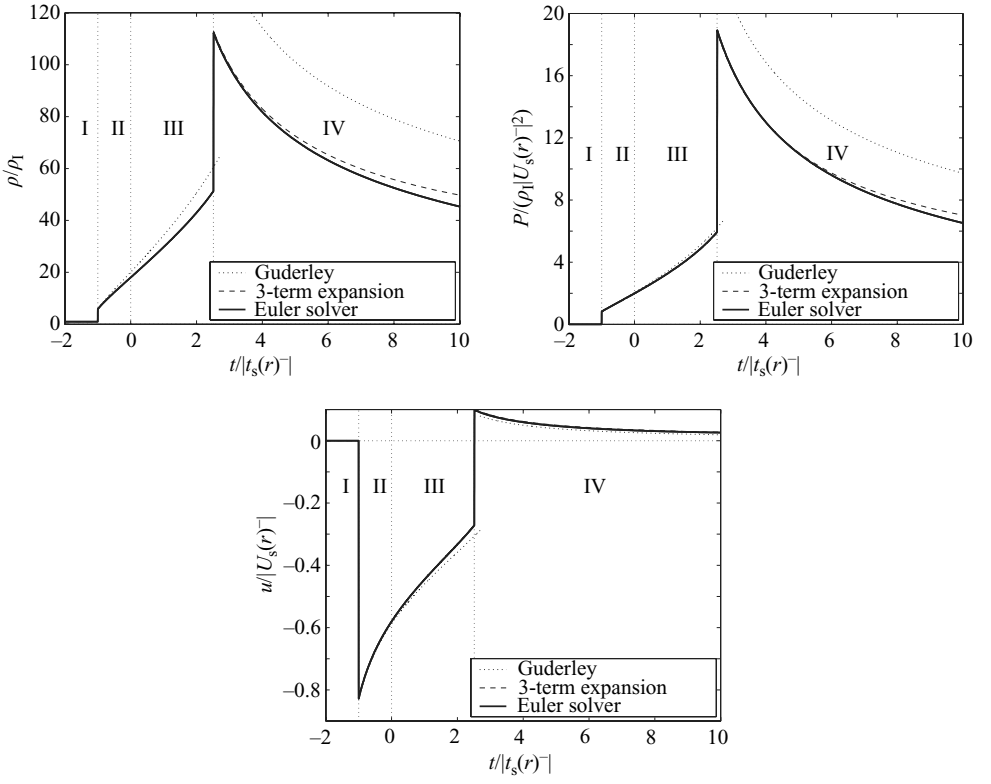


FIGURE 6. Normalized density, pressure, and velocity distributions versus normalized time for a spherical imploding shock ($\gamma = 1.4$). The calculations were started with a shock Mach number of 5 and the measurements were taken at a radius 10 times smaller than the initial radius (where the incoming shock Mach number is 12.4). Note that, although it is sometimes indistinguishable from the Euler computations, the 3-term expansion was plotted in each graph in all the four regions.

strong series expansions of these functions will be compared to the characteristics results and to the Euler solutions. The results will be presented for the axisymmetric case ($\nu = 2$), with a γ of 5/3. The functions F, G and K are represented in figures 7, 8, and 9, respectively. Note that in the reflected shock case, there is no weak-shock series expansion. Also, the characteristics program is only used to compute the incoming shock solution. In all of the figures, the weak-shock series expansion shows very good agreement with the characteristics computation for large radii (or for Mach numbers close to 1). The Guderley solution is excellent for very strong shocks. The addition of two terms to the Guderley solution clearly improves the results since it remains accurate over a wider range of radii.

Discrepancies can be seen in the Euler computations for large $|t|$. This is due to simplified initial conditions and the use of a non-infinite domain. In addition, discrepancies in the Euler solution exist in the region close to the origin because the gradients become very high and numerical error becomes important. Note that even though the initial conditions of the Euler simulation were not perfectly chosen to avoid the introduction of a length scale, the computation quickly converges to the series solution. This suggests that, like the one-term Guderley solution, the series solution is an attractor.

https://doi.org/10.1017/S0022112006000590 Published online by Cambridge University Press

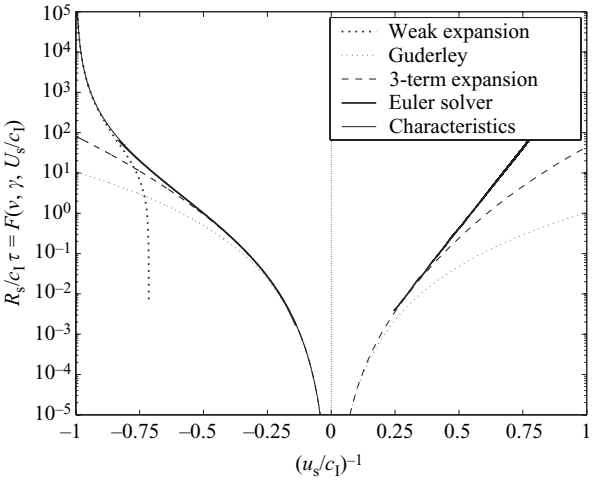


FIGURE 7. Function $R_s/(c_1\tau) = F(\nu, \gamma, U_s/c_1)$ in the axisymmetric case for $\gamma = 5/3$.

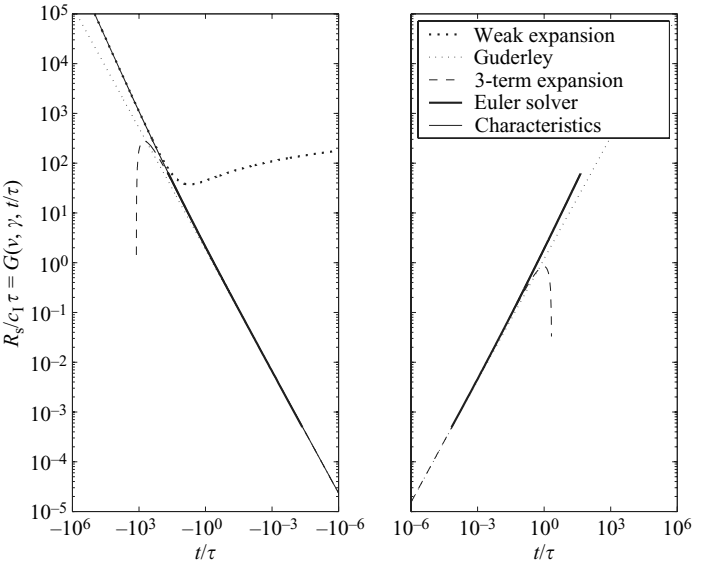


FIGURE 8. Function $R_s/(c_1\tau) = G(\nu, \gamma, t/\tau)$ in the axisymmetric case for $\gamma = 5/3$.

6. Conclusions and future work

In this work, the imploding–reflecting shock problem was investigated with cylindrical and spherical symmetry. The incident shock originated from infinity, travelled through an initially uniform perfect gas at rest, was reflected at the origin, and travelled back to infinity. Guderley's strong-shock solution was expanded using a three-term power series to represent the behaviour of the shock close to the reflection point. Another series expansion was constructed to represent the behaviour of the incoming shock while it is very far from the origin. Finally, the method of characteristics was used to solve the incoming shock problem throughout the entire domain. In order to handle the very large range of radii, an appropriate change of variables had to be made.

https://doi.org/10.1017/S0022112006000590 Published online by Cambridge University Press

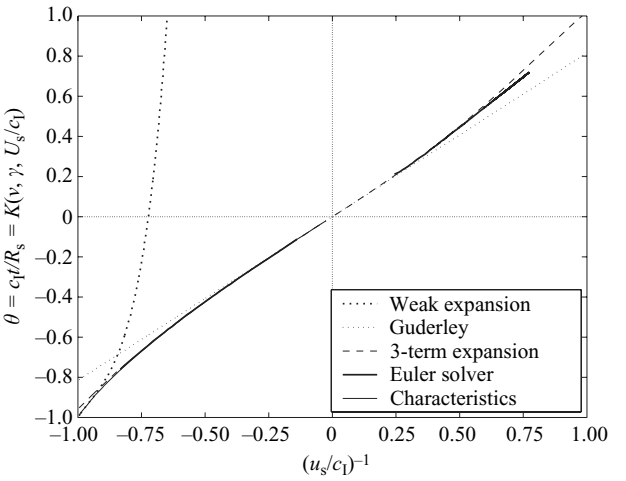


FIGURE 9. Function $\theta = K(\nu, \gamma, U_s/c_1)$ in the axisymmetric case for $\gamma = 5/3$.

Several comparisons between the power series, the method of characteristics, and Euler computation solutions were presented. The results show that the weak-shock expansion series is very accurate for large radii. Also, the two additional terms in the strong-shock series expansion more accurately represent the actual solution around the origin.

The next step to complete this work would be to use the characteristics method to compute the reflected shock motion. This problem is more complicated since both regions around the shock have to be calculated (regions III and IV). In addition, the initial conditions are not based on the strong-shock series expansion since this series is only valid for small r. If the same type of change of variables as the one used in the incoming characteristics program is used for the reflecting part, the following procedure could be used to obtain an initial condition. First, the incoming shock case should be evaluated up to just before the reflection time. Then, the solution at that time has to be transformed back into r–t variables and usual characteristics have to be used to find the evolution of the flow in region II, to cross the boundary between regions II and III, and to continue the calculation up to a small finite positive time. Then, the results should be transformed back into the coordinates used in the characteristics program to form the initial conditions in region III where the radius is sufficiently large that the strong-shock series expansion is no longer accurate.

N.P. and D.P. were partially supported by the Academic Strategic Alliances Program of the Accelerated Strategic Computing Initiative (ASCI/ASAP) under subcontract no. B341492 of DOE contract W-7405-ENG-48.

REFERENCES

CHESTER, W. 1954 The quasi-cylindrical shock tube. *Phil. Mag.* **45**, 1293–1301.

CHISNELL, R. F. 1955 The normal motion of a shock wave through a nonuniform one-dimensional medium. *Proc. R. Soc. Lond.* **232**, 350–370.

CHISNELL, R. F. 1998 An analytic description of converging shock waves. *J. Fluid Mech.* **354**, 357–375.

GUDERLEY, G. 1942 Starke kugelige und zylindrische Verdichtungsstöße in der Nähe des Kugelmittelpunktes bzw. der Zylinderachse. *Luftfahrtforschung* **19**, 302–312.

https://doi.org/10.1017/S0022112006000590 Published online by Cambridge University Press

Hafner, P. 1988 Strong convergent shock waves near the center of convergence: a power series solution. *SIAM J. Appl. Maths* **48** (6), 1244–1261.

Lee, B. H. K. 1967 Nonuniform propagation of imploding shocks and detonations. *AIAA J.* **5** (11), 1997–2003.

Ponchaut, N. F. 2005 Part I: 3DPTV: Advances and error analysis. Part II: Extension of Guderley's solution for converging shock waves. PhD thesis, California Institute of Technology.

Quirk, J. J. 1998 *Amrita – a computational facility (for CFD modeling)*. VKI 29th CFD Lecture Series ISSN 0377-8312.

Whitham, G. B. 1958 On the propagation of shock waves through regions of non-uniform area or flow. *J. Fluid Mech.* **4**, 337–360.

https://doi.org/10.1017/S0022112006000590 Published online by Cambridge University Press